Polymer 50 (2009) 481–490

Contents lists available at ScienceDirect

Polymer

journal homepage: www.elsevier.com/locate/polymer

Large strain behaviour of nanostructured polyelectrolyte hydrogels

Guillaume Miquelard-Garnier, Dominique Hourdet, Costantino Creton*

Physico-chimie des Polymères et des Milieux Dispersés, UMR 7615, UPMC-CNRS-ESPCI, 10 Rue Vauquelin, 75005 Paris, France

ARTICLE INFO

Article history:
Received 22 September 2008
Received in revised form
25 November 2008
Accepted 26 November 2008
Available online 3 December 2008

Keywords:
Gel
Mechanical properties
Hysteresis

ABSTRACT

The mechanical properties of nanostructured polyelectrolyte hydrogels have been investigated targeting specifically the nonlinear deformation regime at large strains and the fracture properties. The hydrogels were synthesized using a thiol-ene cross-linking chemistry of polyacrylic acid precursor chains previously functionalized with double bonds. Some polymers were also grafted with C_{12} side chains able to form hydrophobic clusters in water. The large strain deformation of these nanostructured gels was tested in uniaxial compression by performing loading/unloading cycles at different strain rates and up to different maximum strains. All hydrogels displayed a pronounced strain hardening before fracture and a strain dependent hysteresis but the magnitude of these effects depended on the details of the composition. The most pronounced strain hardening was observed for the unmodified hydrogels in pure water while the largest hysteresis was found for the gels containing the highest concentration of nanoclusters. These dissipative processes barely influence the mechanical behaviour at small strains where the gel remains very elastic but become important at large strains and improve the resistance to fracture of the gels.

1. Introduction

Hydrogels are particularly common in life sciences, food science and can be used for a wide range of applications in engineering [1–3]. They are typically non-toxic and can be manufactured with a variety of different chemistries giving rise to a wide range of physical and mechanical properties.

Although a significant amount of literature is dedicated to the synthesis and swelling properties of hydrogels [4–8] and to the control of their elastic modulus [9–12], less attention has been paid to their large strain properties [13–17] and their resistance to fracture [16,18–21]. Although most hydrogels are soft and fragile materials new routes have been proposed over the past five years for the synthesis of highly swollen and yet remarkably tough gels [20,22,23]. Theoretical arguments based on the behaviour of cross-linked elastomers suggest that for the tougher "double network" gels, finely tuned dissipative mechanisms at the crack tip cause this enhanced toughness at high deformation [24,25]. However a general explanation for the toughness of hydrogels is still lacking.

One of the possible routes to synthesize dissipative hydrogels can be inferred from the behaviour of nanomaterials such as rubbers filled with inorganic particles. Pure well-cross-linked rubbers are typically not very tough and fail at relatively low extensions. However, when small filler particles, such as carbon black, are added to the rubbers, their fracture toughness increases significantly [26,27]. It is widely believed that this toughening mechanism is due to the existence of a percolating network of weaker interactions between the particles that can break at large strains before any covalent bond is broken.

This idea can be transposed to hydrogels by several methods. One of them is the use of associating-water soluble polymers [28–31]. These amphiphilic macromolecules contain a main hydrophilic part that maintains the solubility of polymer chains in water as well as hydrophobic moieties which provide the associative behaviour. Once dissolved in water, these polymers self-assemble and form a transient network with hydrophobic clusters connecting hydrophilic chains [32]. These temporary associations of hydrophobic groups dramatically increase the viscosity of the solution [31,33] and have been modelled as polymer chains carrying a small amount of sticker groups [34].

By chemically cross-linking water-soluble associating polymers [35], a hydrogel with both permanent and reversible junctions can be formed [36]. If the hydrophobic clusters have a lifetime of the order of the inverse of the strain rate, they are expected to induce dissipative mechanisms in the hydrogel, so that its mechanical properties and especially its loss modulus and hysteresis during loading unloading cycles should be increased.

In a first article [29] we described a possible route to prepare such materials by chemically cross-linking with dithiols hydrophobically modified poly(sodium acrylate) functionalized with double bonds [37,38]. The rheological behaviour of these systems was also reported and we showed that the elastic and the loss

* Corresponding author. Tel.: +33 140 79 46 83; fax: +33 140 79 46 86.
E-mail address: costantino.creton@espci.fr (C. Creton).

0032-3861/$ – see front matter © 2008 Elsevier Ltd. All rights reserved.
doi:10.1016/j.polymer.2008.11.045

modulus could be independently controlled by the gel concentration and by the density of hydrophobic groups, respectively. G'' was increased by two orders of magnitude compared to the unmodified hydrogel showing dissipation, due to the hydrophobic clusters, at small strains, i.e. in the elastic region.

In a second paper [17], we presented results of uniaxial compression–decompression experiments at large strains for "model" polyelectrolyte hydrogels (without alkyl groups) synthesized by the method presented previously. We identified for these hydrogels an early strain hardening as well as a significant strain dependent hysteresis which were not due to an irreversible fracture of the gel structure. These effects were attributed to strain-induced polyelectrolyte physical aggregation.

In the present paper we focus on the large strain properties of hydrophobically modified polyelectrolyte hydrogels using the same uniaxial compression tests. Since the presence of these hydrophobic nanoclusters markedly increased the viscoelastic behaviour of the gel in the linear regime of deformation [29], it was plausible that their presence would also enhance dissipative processes in the large strain regime. We also demonstrate that these dissipative mechanisms lead to an increase in fracture toughness of the gels.

2. Experimental part

The synthesis of the polymer precursors and hydrogels as well as the preparation of the samples for the mechanical tests was described in details in previous papers [17,29] so we will only summarize the most important steps here.

2.1. Materials

2.1.1. Polymer precursor

Poly(acrylic acid) (PAA) was obtained in its acid form from Aldrich. Its number average molecular weight as characterized by size exclusion chromatography (SEC) was $M_n = 35$ kg/mol ($M_w/M_n \approx 10$).

2.1.2. Modification of PAA

PAA chains were submitted to different chemical modifications. All the polymer chains were initially modified by introducing a given proportion of double bonds (allylamine) along the backbone, in order to create cross-linking sites. In addition some of them were also modified with different proportions of short hydrophobic chains (dodecylamine). Both reactions were carried out in NMP (N-methyl-2-pyrrolidone) by grafting amino terminated molecules (allylamine and dodecylamine) onto the carboxylic acids of the polyacrylic backbone in the presence of dicyclohexylcarbodiimide (DCCI) which activates the formation of amide bonds. These reactions are quantitative and the distribution of the grafts can be considered as random. Three different polymers were synthesized with 10 mole% of double bonds and various molar amounts of C_{12}: 0, 3 and 5%. These three polymers, obtained under their sodium salt form, will be referred to as PAA10 db, PAA3C12 and PAA5C12, respectively.

2.1.3. Synthesis of the hydrogels

The cross-linking reaction was carried out in water, at room temperature and under atmospheric conditions. Modified PAA, dithioerythritol (bifunctional thiol) and KPS (potassium peroxodisulfate) were separately dissolved in water at the desired concentration (KPS and dithioerythritol are always used in stoechiometric conditions compared to the initial number of double bonds added). All concentrations, for solutions and gels, are expressed in percent w/w.

The KPS was then added to the PAA solution under stirring and finally dithioerythritol was quickly added into the solution. After an energetic stirring during a few seconds, the solution was finally left to rest for gelation.

The gels were always tested at their preparation concentration, far from the equilibrium swelling (for a 6% hydrogel, the swelling ratio is $Q \approx 16$ whereas at equilibrium $Q_e \approx 90$. These values do not depend on the presence of alkyl groups).

As the pH of a solution of modified PAANa is around 7 in our range of concentrations and the pK_a of acrylic acid is 4.2, the proportion of charged monomers along the backbone can be estimated close to 1.

Complementary experiments were made with the same gels swollen *N*-methyl pyrrolidone (NMP) [17]. The gels were prepared in water first. The PAANa was then converted to its acid form by deswelling it gently in an excess of HCl solution. After several rinses with ethanol to eliminate the NaCl salt formed, the gel was then dried slowly at room temperature (the drying was controlled by sample weighing). When the gel was dry, it was swollen in NMP at the desired concentration. To study identical gel structures in both solvents, the molar concentration of polymer was kept constant for both water and NMP.

2.1.4. Compression tests

The experiments were performed on a custom designed mechanical tester [39] with a force resolution of 0.01 N and a displacement resolution of 0.1 μm, which is adapted to the testing of small and soft samples. In order to avoid adhesion between the gel and the surfaces, a thin layer of dodecane was present on the surfaces of the gel and on the glass slides. Further details on the sample preparation and geometry have been previously described [17].

A typical compression test consists of an initial compressive contact to −0.03 N. This initial compressive value ensures a reproducible starting point of complete contact between the gel and glass surfaces. Below this level of deformation, the adhesive forces causing a jump in contact and the lack of parallelism between the probe and the gel resulted in an irreproducibility of the results. This procedure ensured values of the initial gel modulus in quantitative agreement with the rheological measurements obtained previously [29]. Unfortunately, with this procedure, the non-deformed and small deformations data (λ close to 1) are not collected.

The test then begins with a compression step performed at a constant crosshead speed (10 μm s^{-1}, 50 μm s^{-1} or 200 μm s^{-1}) to a preset maximum load (varied between 0.5 and 10 N corresponding to true stresses varying from 6.5 kPa to 75 kPa), followed by immediate retraction to the zero displacement at the same speed and a wait time (about 1 min), until the next cycle of compression. Some experiments were also performed at 1 μm s^{-1} and 600 μm s^{-1}.

Relaxation experiments were also performed on the same apparatus: the gel was brought into contact with the glass slide to a point of maximum compression at high speed (200 μm s^{-1}, meaning that it took roughly 5–10 s to bring the gel to its maximum compression). The displacement was then kept constant for a certain time (typically 3600 s), and the gel was left to relax. Force and time data were collected.

Fig. 1 shows schematically the compression test on the macroscopic gel sample as well as a molecular picture of the chain deformation. a_0 is the initial radius of the gel cylinder. The parameter λ is defined as the compression ratio in the z-direction, $\lambda = h/h_0$, where h_0 is the initial height of the gel cylinder and h its current height.

Since the gel behaves as an elastomer, it deforms at constant volume and it is useful to define:

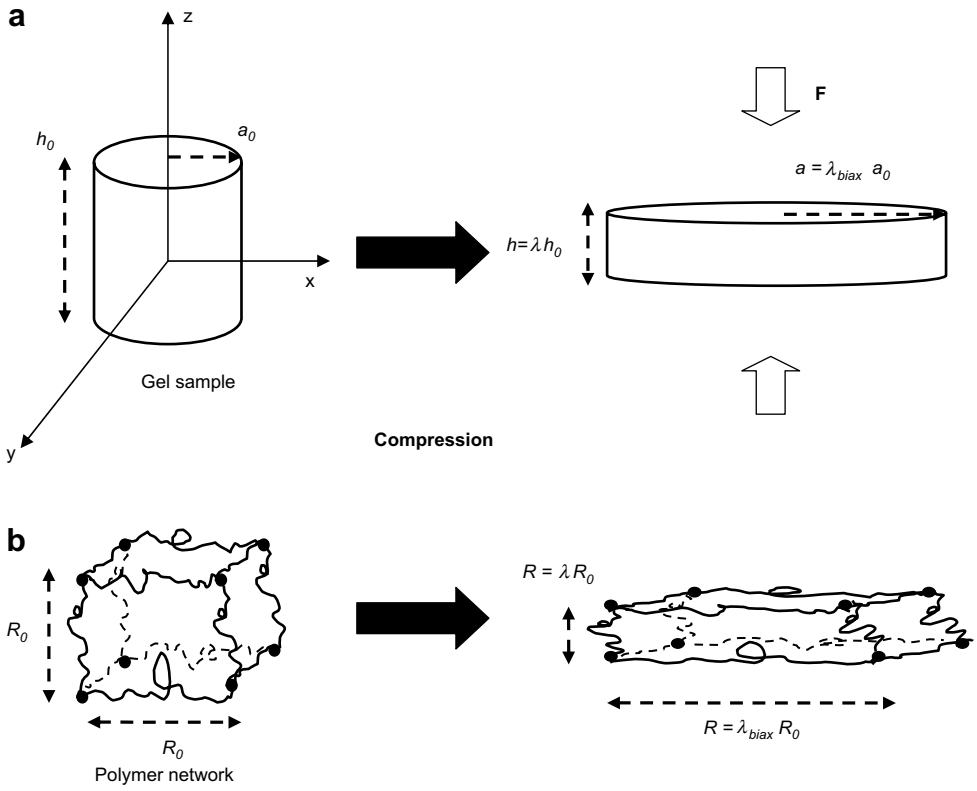

Fig. 1. a. Schematic representation of a compression test on a gel sample. b. Schematic representation of a compression test on the polymer network based on an affine deformation.

$$\lambda_{\text{biax}} = \frac{1}{\sqrt{\lambda}}. \quad (1)$$

Assuming an affine deformation for the network, we can see that compression in the z-direction is causing an orientation of the chains in the x–y plane ($\lambda_{\text{biax}} > 1$ and increases with deformation) whereas their radius of gyration decreases in the z-direction ($\lambda < 1$ and decreases with deformation). With these experiments, we are performing a uniaxial compression test equivalent to a biaxial extension in the plane normal to the loading direction.

In the following, some of the results obtained are best understood as an effect due to the extension of the chains in the x–y directions, while others are more intuitively due to the compression in the z-direction. In consequence, depending on their molecular origin, the effects observed will be presented as a function of the most relevant parameter λ or λ_{biax}.

2.1.5. Fracture tests

Preliminary fracture experiments in pure shear geometry [40] were also performed. The setup was custom designed, based on the work of Baumberger et al. [19,41]. In order to work on few mL samples, a miniaturized Plexiglas mould was built ($100 \times 20 \times 1$ mm). Each face of the mould can be separately removed (see Fig. 2). A Velcro is glued to the up and down sides in order to hold the gel film.

After a rapid stirring of the KPS, dithioerythritol and PAA, the solution was poured in the mould which was then closed until the gel was fully formed. To help the demolding, a silicone lubricant was used on the sidewalls of the mould. Prior to the fracture tests,

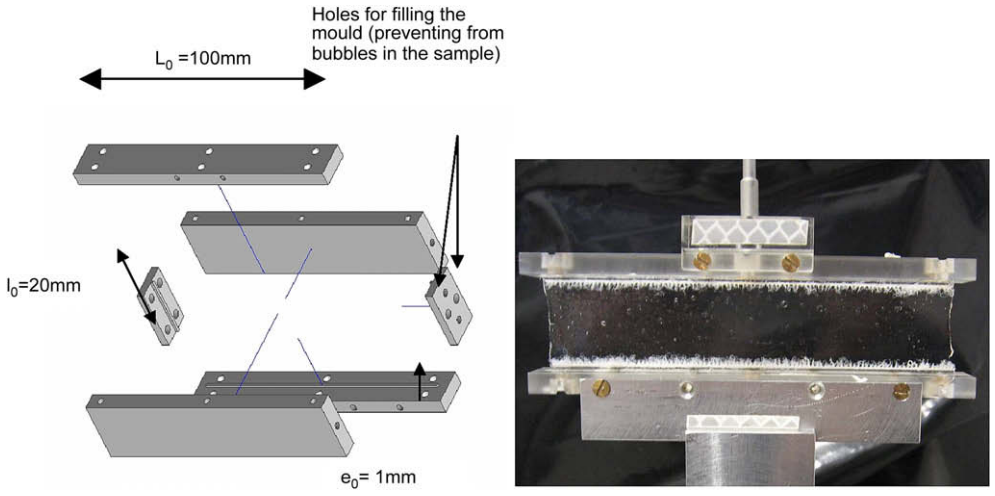

Fig. 2. Schematic representation of the fracture mould and picture of a sample: the gel is fixed to the upper and lower side of the mould by a Velcro strip. The sample is fixed to the tensile testing machine.

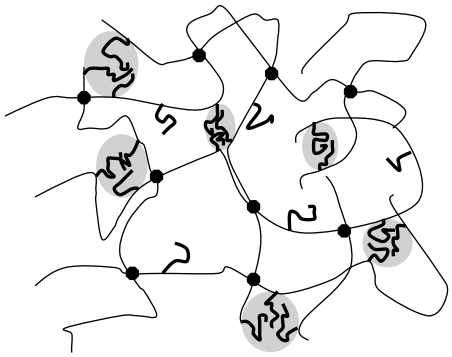

Fig. 3. Schematic structure of the hydrophobically modified hydrogel.

the samples were notched at one edge to initiate the crack. The notch was typically a few mm long in these experiments.

The fracture tests were carried out on a JFC TC3 machine fitted with a 10 N load cell and a resolution of ±0.5 mN. The crosshead speed was kept constant at $v \approx 15\,\mu m\,s^{-1}$ leading to a strain rate $\dot{\varepsilon} \approx 7.5 \times 10^{-4}\ s^{-1}$, with a resolution of 0.01 mm.

3. Results

3.1. Structure of the hydrogels

The structure of the hydrophobically modified hydrogel [29] can be schematically described in Fig. 3.

PAA chains are chemically cross-linked (small filled circles) by the reaction of dithioerythritol with the double bonds and physically cross-linked by hydrophobic micelles (grey clusters). Thiol titration experiments coupled with elastic modulus measurements showed that the thiol-ene reaction was far from complete and only 2–12% of the double bonds give rise to interchain cross-links (whereas roughly 40% create intramolecular loops). In consequence, assuming a Gaussian conformation of the chains, the distance between two cross-links can be roughly estimated to 100–200 Å, depending on the polymer concentration [29]. For a 5% polymer concentration this gives on average one cross-link per chain but it should be noted that the molecular weight distribution of the PAA starting polymer is very wide and the network is probably formed mainly by the long chains at that concentration. Hydrophobic micelles (grey) are dispersed in the network, whereas some C_{12} chains (bold) remain in a non-aggregated state. The ratio aggregated/free alkyl groups increases with increasing concentration of polymer and increasing concentration of alkyl groups (i.e. at the same polymer concentration, PAA5C12 hydrogels have a higher fraction of embedded C_{12} than PAA3C12, and the same holds when increasing the polymer concentration in the gel). The hydrophobic clusters were characterized by SANS and ^{13}C NMR and their radius was estimated around 18 Å (aggregation number ~ 70) [29].

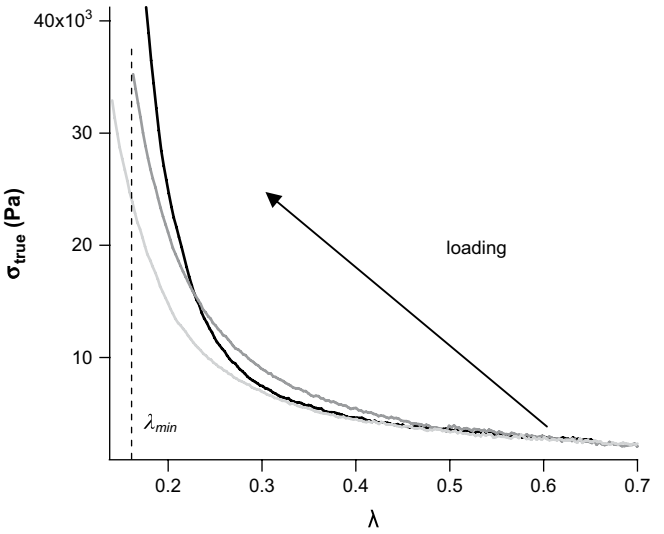

Fig. 5. True compressive stress versus compressive lambda for PAA10 db (black), PAA3C12 (dark grey) and PAA5C12 6% (light grey) gels (maximum force applied = 5 N, crosshead speed 50 $\mu m\,s^{-1}$). Fig. 5 also shows an example the minimum compressive lambda λ_{min} reached during the test by the PAA3C12 hydrogel.

We showed by DSC (Differential Scanning Calorimetry) and titration measurements that the kinetics and the yield of the chemical gelation process were not affected by the presence of the hydrophobic groups.

At small deformations (1%, 1 Hz), the hydrophobically modified hydrogels (PAA3C12 and PAA5C12) displayed identical elastic moduli G' (controlled only by the total polymer concentration in the gel) to those of the unmodified reference PAA10 db. On the contrary, a large increase of the loss moduli G'' (by two orders of magnitude) is observed for the hydrophobically modified hydrogels. Interestingly this difference is apparent as soon as the clusters are present in the gel, while the difference between 3C12 and 5C12 is relatively modest [29].

3.2. Mechanical results

3.2.1. Strain hardening and maximum extensibility

The goal of this paper is to investigate the role of the hydrophobic clusters in the dissipative mechanisms that occur in the gel

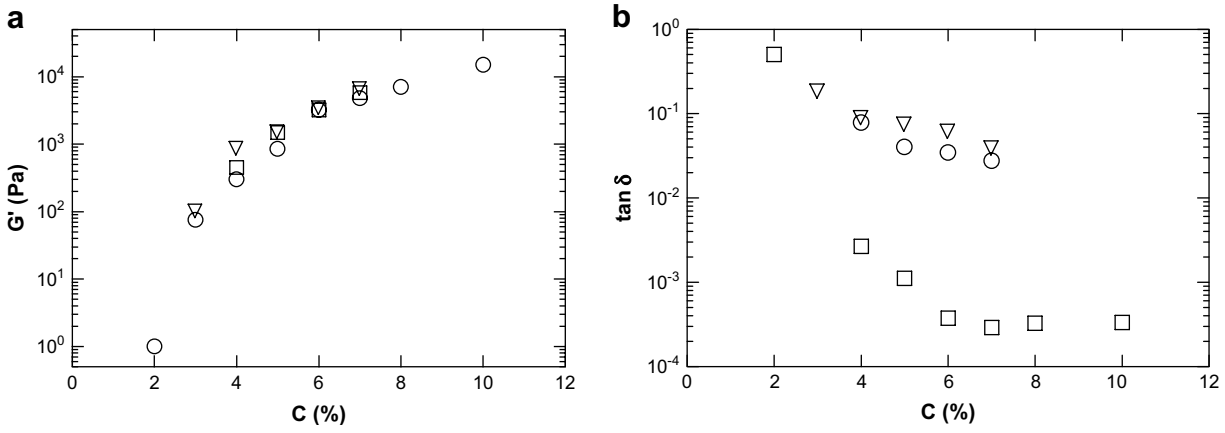

Fig. 4. a. Evolution of the storage modulus for PAA10 db (□), PAA3C12 (○) and PAA5C12 (▽) as a function of the concentration and b. evolution of the loss factor tan δ ($\gamma = 1\%$, $f = 1$ Hz).

at large compressive strains, as they compete with dissipative mechanisms induced by strain-induced physical aggregation previously identified for the PAA10 db hydrogels [17].

Fig. 5 shows a typical stress-lambda curve from a compression test trial at 5 N for PAA10 db, PAA3C12 and PAA5C12 gels at 6% w/w but similar results were obtained at other concentrations[1]. We plotted the true stress defined as $\sigma_{true} = -(F/\pi a_0^2)\lambda$, where F is the experimental compressive force.

The following observations can be made from Fig. 5.

1. The three gels roughly have the same small strain elastic modulus, consistent with the values obtained from rheology [29]. By fitting the small strain data, G can be estimated for the three gels around 3 kPa ± 150 Pa which is really close to the values obtained by rheological measurements for 6% hydrogels [17].
2. The strain hardening observed at large strains is more progressive for the hydrophobically modified gels compared to the unmodified gels where it appears suddenly and increases very sharply. In consequence the maximum extensibility is higher for hydrophobically modified hydrogels than for the PAA10 db gels. This effect is increased with increasing quantity of micelles in the gel (since there are more hydrophobic micelles in the PAA5C12 than in the PAA3C12 at the same polymer concentration) [29].

The large strain behaviour of elastic networks can be quantitatively analyzed with an empirical model developed by Gent for unentangled cross-linked networks undergoing strain hardening at large strains [42]. This model introduces the maximum extensibility of the network chains in the material through a maximum value of the first strain invariant where the strain energy function diverges. Since a maximum extensibility of the network chains is a counterintuitive concept for uniaxial compression tests, we have represented the data in Fig. 5 as a function of the biaxial strain in the plane normal to the compression direction. The governing equation relating true stress and biaxial stretching within the framework of the Gent model is [14,42]:

$$\sigma_{true} = G\frac{\lambda_{biax}^2 - \lambda_{biax}^{-4}}{[1-(J_1/J_m)]} \quad (2)$$

where G is the shear modulus, J_1 is the first stress invariant for simple extension in the 1-direction (equal to $\lambda_1^2 + 2\lambda_1^{-1} - 3$, with $\lambda_1 = \lambda$ in our tests), and J_m is an adjustable parameter representing finite extensibility as a maximum allowable value for the first stress invariant. G and J_m are the two adjustable parameters for the fits.

The results, presented in Fig. 6 and summarized in Table 1, show that the Gent model fits fairly well the shape of the strain hardening curves for our hydrogels, hydrophobically modified or not.

We can see on this graph and in Table 1 that J_m which is directly related to the maximal experimental finite extensibility [42] increases with decreasing concentration for both gels.

For unmodified gels, we found that the experimental values were much lower than what could be predicted from simple models of finite extensibility of Gaussian chains or of concentrated polyelectrolyte chains [17]. These differences between theory and experiment for unmodified hydrogels were interpreted in our preceding paper as being due to a strain-induced formation of ionic clusters acting like additional physical cross-links in the course of deformation.

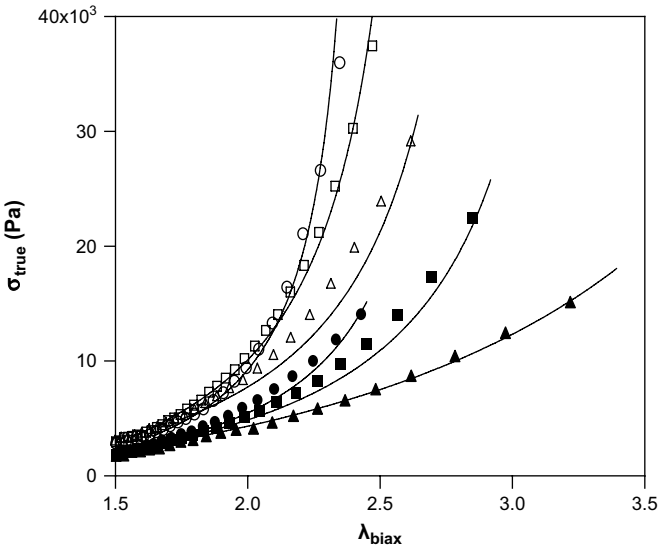

Fig. 6. True stress versus biaxial lambda for PAA10 db (circles), PAA3C12 (squares) and PAA5C12 (triangles) hydrogels at 5% (full symbols) and 6% (open symbols) with corresponding Gent fits (full lines) ($v = 50\ \mu m\ s^{-1}$ corresponding to 0.013–0.016 s^{-1} depending on sample initial size).

Interestingly, the J_m values measured for the hydrophobically modified gels are significantly higher and closer to the theoretical predictions for a network of Gaussian chains of identical small strain modulus, especially for the PAA5C12. This suggests that:

- the presence of hydrophobic clusters inhibits the formation of ionic aggregates between charged chains.
- the hydrophobic clusters do not prevent the extension of network chains and do not appear to act as additional topological constraints at least at long times.

3.2.2. Strain rate effects on the stress–strain behaviour

The large observed hysteresis suggests that it will be instructive to compare the strain rate effects on the loading behaviour of the modified and non-modified gels. In consequence, samples of the same material at the same polymer concentration were compared at different actuator speeds, varying from 1 $\mu m\ s^{-1}$ to 600 $\mu m\ s^{-1}$, corresponding to an initial strain rate varying from $0.29 \times 10^{-4}\ s^{-1}$ to $1.7 \times 10^{-1}\ s^{-1}$, respectively, for an initial sample height of 3.5 mm (note that the time of the experiment is consequently varying roughly from 3600 s to 5 s, a range of times where drying effects were checked to be negligible for our setup).

Repeating these experiments for several systems and concentrations, it is possible, using the Gent fits, to obtain the value of J_m for different strain rates. For all systems and the concentrations studied, J_m increases slightly with decreasing strain rates, as presented in Fig. 7.

Fig. 7 shows clearly a rate dependence of the maximum extensibility parameter for both modified and unmodified gels. As the strain rate is reduced, the strain hardening becomes less pronounced. Interestingly, a significant difference was found between the behaviour of the 3C12 and 5C12, while at small strains (Fig. 4), the difference is much more marked between the 10 db and the two modified polymers.

3.2.3. Hysteresis energy

The third important point in the set of compression experiments was the significant hysteresis observed between the loading and the unloading curves.

[1] When comparisons are needed, in most cases, the 6% concentration will be used since it is the best compromise for the three systems (for concentrations higher than 7%, the viscosity of the PAA5C12 solutions is too high to synthesize homogeneous hydrogels, whereas for concentrations below 5%, the systems are too close to their percolation concentration).

Table 1
Fitted values of J_m for the different gels.

C	5%			6%			7%		8%	
Type of gel	10 db	3C12	5C12	10 db	3C12	5C12	10 db	3C12	10 db	3C12
J_m	**15.2**	**21**	**50**	**10.1**	**13.4**	**23.2**	**7.3**	**10**	**6.6**	**9.1**
Standard deviation from the fit on a given sample	±0.2	±1	±5	±0.1	±0.1	±0.5	±0.05	±0.1	±0.05	±0.1
Standard deviation between different samples	±2	±3	±5	±2	±2	±4	±1	±2	±1	±1

Fig. 8a shows that the hysteresis becomes significant only when a critical deformation is reached ($\lambda_{3C12\ 6\%} \sim 0.4$ from Fig. 8a). This threshold was already identified for unmodified polyelectrolyte hydrogels [17]. The hysteresis is highly strain dependent. However it is difficult to extract a more quantitative comparison since for the hydrophobically modified hydrogels the hysteresis is due to the reversible formation of both ionic and hydrophobic clusters and the respective importance of the two mechanisms will depend on strain rate.

In Fig. 8b, we can see that the level of hysteresis increases with increasing density of hydrophobic clusters.

It is now worthwhile to explore further the possible physical causes of the hysteresis.

As shown in Fig. 9 where two successive compressions have been applied to a PAA3C12 hydrogel ($C = 6\%$, $F = 5$ N) no permanent damage results from the hysteretic behaviour. This result, found for all three gels, is in sharp contrast with what was found for the tough double network hydrogels developed by the Gong group [20,21].

The hysteresis for each experimental condition, or energy dissipated, was then quantified according to the following equation:

$$E_{hyst} = \int_{loading} \sigma_{comp} d\varepsilon \int_{unloading} \sigma_{comp} d\varepsilon \quad (3)$$

where σ_{comp} is the nominal stress and ε is the nominal strain of the stress–strain curves.

Since we showed earlier, that the fitted maximum extensibility J_m (for a given strain rate) is a material characteristic different for each material and strain rate, it is reasonable to define a reduced deformation as:

$$\lambda_{red} = \frac{\lambda_{biax} - 1}{\lambda_{biax,m} - 1} \quad (4)$$

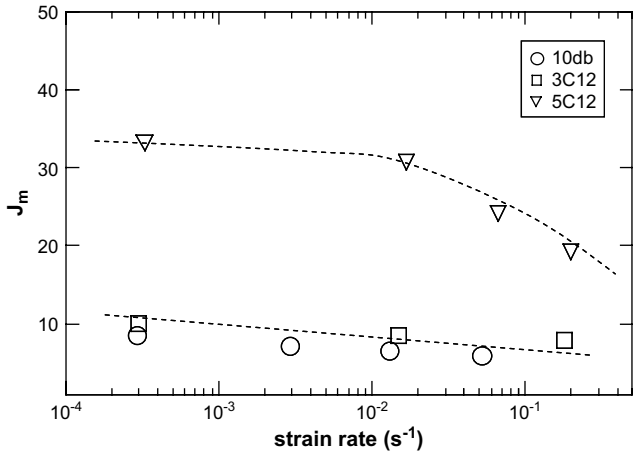

Fig. 7. Strain rate effects on the stress–strain behaviour of hydrogels. Fitted value of J_m as a function of strain rate for several systems (maximum force applied: 1 N for PAA10 db and PAA3C12, 2 N for PAA5C12).

where $\lambda_{biax,m}$ is the maximal biaxial lambda value obtained from the Gent fits of J_m ($\lambda_{biax,m} \approx \sqrt{J_m + 3/2}$) [17,14].

The reduced deformation λ_{red} is then 0 in a non-deformed state and 1 when the extensibility is equal to its maximum value obtained using the Gent fits. We use it here to separate the effect of ionic aggregates (which mainly affect the finite extensibility) from that of the hydrophobic clusters (mainly affecting dissipation).

Plotting the hysteresis as a function of λ_{red} (see Fig. 10), two contributions can be clearly identified with this graph. The first contribution appears at high strains ($\lambda_{red} > 0.6$) for non-hydrophobic gels. As these gels are fully elastic ($G' \sim 10^3\ G''$) at small strains, this hysteresis was attributed to a strain-induced formation of dynamic ionic clusters in the gel which stiffen the gel during loading and disappear with a delay during unloading [17].

Another dissipative process appears at lower strains ($\lambda_{red} \sim 0.3$ for PAA5C12, $\lambda_{red} \sim 0.4$ for PAA3C12) and seems to be clearly related to the presence of hydrophobic clusters in the gel.

Similarly to the small strain dissipation measured by G'', the level of hysteresis increases as the density of clusters increases. Since the size of the hydrophobic clusters does not appear to change much with concentration of hydrophobic groups [29], it is interesting also to represent the hysteresis energy as an energy dissipated per cluster rather than per unit volume. Following the same procedure as in Ref. [29], we represented in Fig. 10b, the hysteresis energy per cluster. Although one cannot really speak of a master curve it is clear that a more universal behaviour is observed and the energies dissipated can becomes quite large. Given that each cluster contains an average of about 70 chains [29] the energy can be as high as 10 kT per chain, clearly sufficient to breakup a cluster.

3.2.4. Rate effects on the hysteresis

Similarly to the strain hardening, the hysteresis is also influenced by the strain rate.

Since this effect was observed to a certain extent for all types of gels [17], the hysteresis was studied at different strain rates, in order to identify how it affects the relaxation behaviours of the two types of clusters.

The same compression experiments were performed for various gel concentrations at increasing initial strain rates ($10\ \mu m\ s^{-1}$, $50\ \mu m\ s^{-1}$ or $200\ \mu m\ s^{-1}$ corresponding to $\approx 3 \times 10^{-3}\ s^{-1}$, $1.4 \times 10^{-2}\ s^{-1}$ and $5.6 \times 10^{-2}\ s^{-1}$, respectively) and hystereses were measured. These experiments were carried out at several maximum force values for PAA10 db and PAA3C12 hydrogels at 6%. The values obtained for the hysteresis energy as a function of the reduced lambda are presented in Fig. 11a.

In Fig. 11b, several samples were brought to the same minimum compressive lambda λ_{min} (see Fig. 5) at different strain rates and hysteresis was measured.

Fig. 11a shows a significantly larger rate effect on the hydrophobic modified hydrogels than on the simple PAA gel. Fig. 11b shows that this rate effect is particularly important in the case of the cluster-rich PAA5C12. These two graphs suggest strongly that the two respective mechanisms identified for the hysteresis are both strain rate dependent but with very different characteristic time scales.

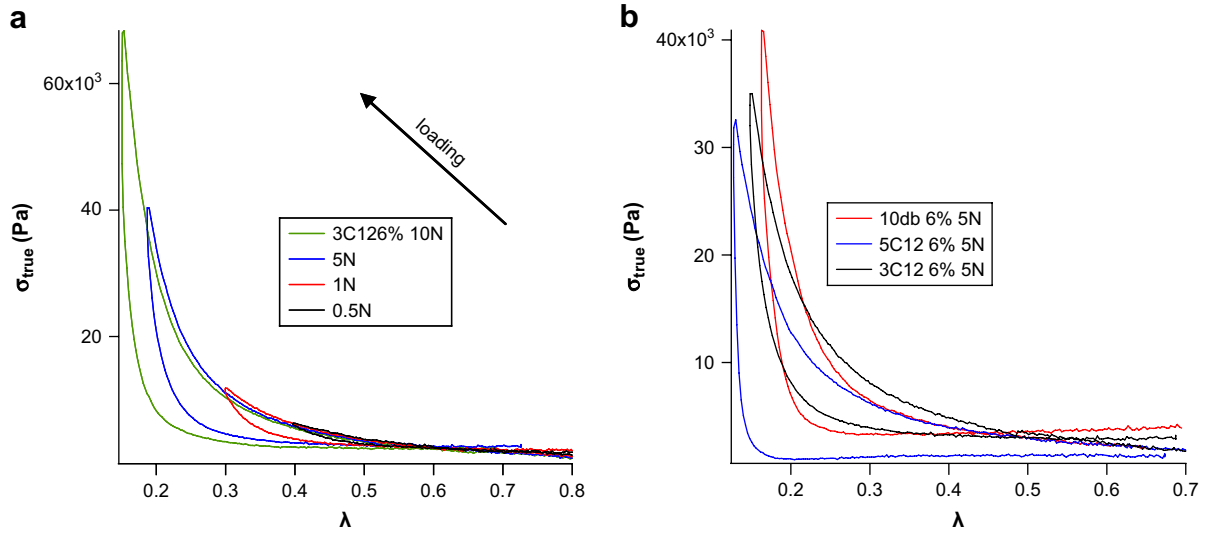

Fig. 8. a. True stress versus compressive lambda for PAA3C12 6% at different maximum compressive force values. b. True stress versus compressive lambda for PAA10 db (red), PAA3C12 (black) and PAA5C12 (blue) 6% gels (maximum force applied = 5 N, crosshead speed 50 $\mu m\,s^{-1}$) (For interpretation of the references to colour in this figure legend, the reader is referred to the web version of this article).

3.2.5. Stress relaxation

The existence of two distinct time scales for the dynamics of the gels at large strains was confirmed by more standard relaxation experiments. Two characteristic relaxation times were observed for the pure PAA10 db hydrogels [17]. The first one around 10 s and the second one of the order of 1500–2500 s.

The graph presented in Fig. 12a shows the stress relaxation ($\sigma_{true}/\sigma_{true0}$) as a function of time for different maximum compressive strains for the three types of gels. σ_{true0} is the true stress observed at $t = 0$ which is the point when the maximum compression is reached, i.e. the minimum compressive lambda λ_{min}. The same results are presented in Fig. 12b in a normalized fashion to extract the contribution of the hydrophobic clusters only. Given the time it takes to reach the maximum compressive strain, the first 10 s of the relaxation is difficult to analyze and will be ignored.

First, it is clear by looking in Fig. 12 that the contribution of the hydrophobic clusters in the relaxation processes increases with increasing hydrophobic content. But the most important feature is that the lifetimes of the two types of clusters are very different, higher than 1000 s for the ionic clusters (observed for all gels) and around 150–200 s for the hydrophobically modified ones. This was already suggested by the different strain rate effects observed on the hystereses. Fig. 12b also implies that at long times the clusters do not influence the relaxation processes, since the difference between the stresses reach a constant value for times higher than 500 s.

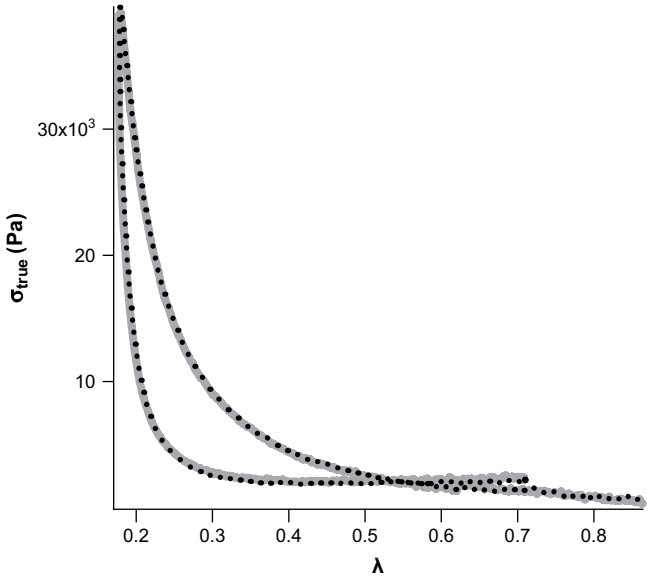

Fig. 9. Successive compressions at 2 min interval (first: grey curve, second: black dotted line) for a PAA3C12 6% hydrogel ($F = 5$ N).

3.2.6. Solvent effects

Many of our interpretations are based on the existence of associations between molecules in water either due to charge effects or to a poor solubility of hydrophobic groups. If the gels are swollen in a good common organic solvent these effects should disappear. The same compression experiments were hence performed on gels swollen in NMP since both PAA under its acid form and C_{12} groups are soluble in these conditions.

As shown in Fig. 13, all the different gels display a very similar mechanical behaviour when swollen in NMP. Strain hardening and hysteresis are much less pronounced for the NMP-gels, as one would expect from a classical elastic network (J_m close to what is expected for a Gaussian network, in the range of 50–100).

3.2.7. Enhanced mechanical strength

The dissipative mechanisms induced by the presence of the hydrophobic clusters enhanced somewhat the resistance to fracture of the hydrophobically modified hydrogels compared to their unmodified counterparts PAA10 db. However, because the hydrophobic clusters make them softer at large strains, the main effect is that of a larger extensibility before fracture, but the fracture true stress does not increase by more than a factor of two.

If a pure shear sample is used to study crack propagation [40,41] all samples fracture in a brittle fashion and the force-strain curves are presented in Fig. 14.

Using the pure shear geometry equations classically used for fracture of cross-linked rubbers [40], we can estimate the energy

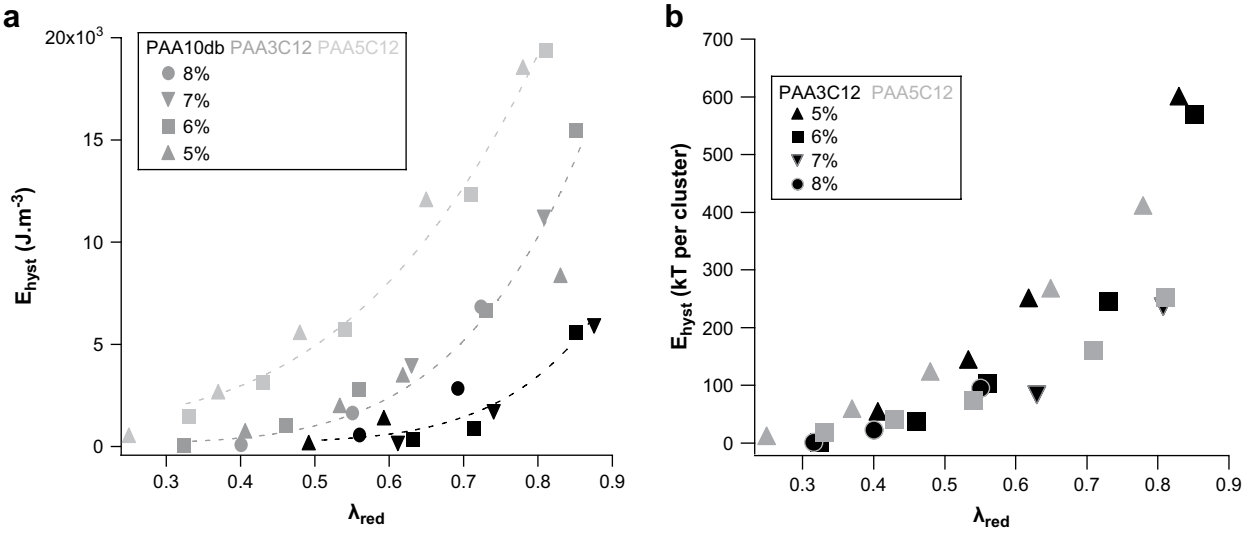

Fig. 10. a. Hysteresis per unit volume of gel versus λ_{red} for the three gels at several concentrations. b. Hysteresis per cluster as a function of λ_{red} for the PAA3C12 and PAA5C12 at different concentrations.

release rate G as a function of the stress level by integrating the curves presented in Fig. 14.

$$G_c = \frac{h_0}{L_0 e_0}\int F\,d\varepsilon = h_0\int \sigma_{comp}d\varepsilon \quad (5)$$

However, edge effects can lead to an underestimate of the stored elastic energy (close to the edge, the sample is in fact in uniaxial traction and not in pure shear. These two approximations lead to a range of values for different samples:

PAA10 db 5%: $G_c h \approx 1.5$–3 J/m^2 PAA5C12 5%: $G_c h \approx 6.5$–11 J/m^2
PAA10 db 6%: $G_c h \approx 2.5$–5 J/m^2 PAA3C12 6%: $G_c h \approx 7.5$–12 J/m^2

The modified gels give systematically higher experimental values for G_c. However, the hydrophobic micelles only lead to a moderate mechanical toughening of the hydrogels with G_c values remaining much lower than what has been observed for gelatine gels [19] at high crack velocities or for double network gels [20].

4. Discussion

Hydrophobically modified polyelectrolyte hydrogels display significant dissipative mechanisms when deformed at large strains. By analyzing the experiments, it appears that these dissipative mechanisms are at least of two types.

The first one is due to the polyelectrolyte network which can create a progressively percolating network of ionic aggregates when a critical deformation is reached [17]. This strain-induced clustering of ionic aggregates causes an important strain hardening, a large hysteresis in the loading/unloading curves and a stress plateau during unloading. These clusters have a rather long relaxation time of the order of 10^3 s. The second dissipative mechanism is due to the formation of a transient network of hydrophobic micelles formed in the hydrogel. These two phenomena are strongly coupled and difficult to study separately.

What can be said by analyzing the loading/unloading compression curves is that the presence of the hydrophobic clusters seems to screen the interactions responsible for the formation of the ionic clusters. At a given strain rate, the strain hardening is

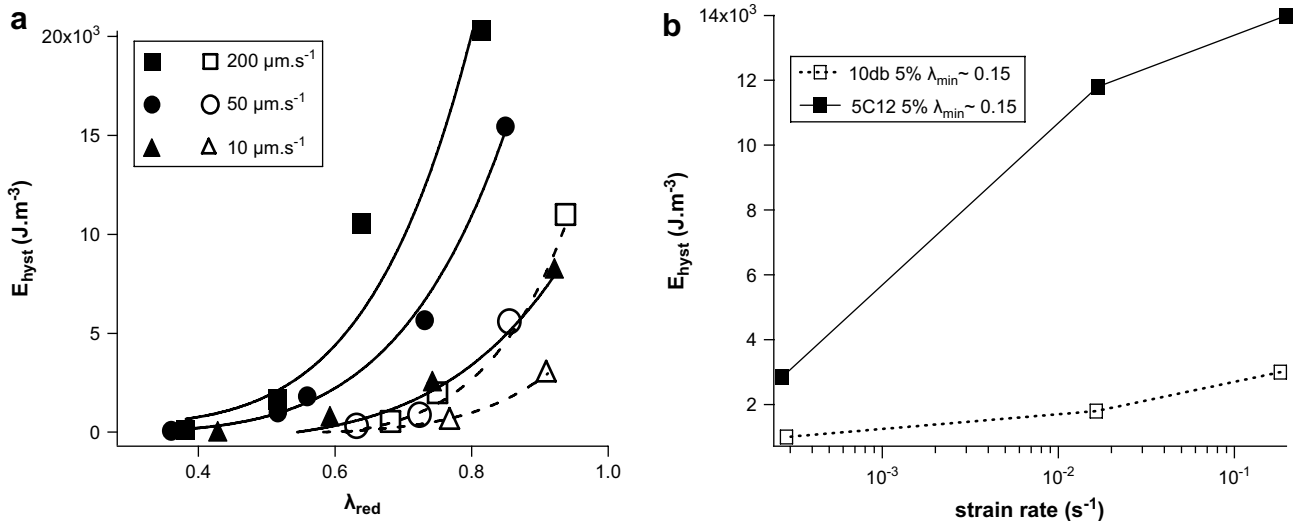

Fig. 11. a. Hysteresis energy versus reduced lambda for 6% hydrogels (10 db: open symbols, 3C12: full symbols) at several compression rate values b. hysteresis energy versus strain rates for a given minimum lambda.

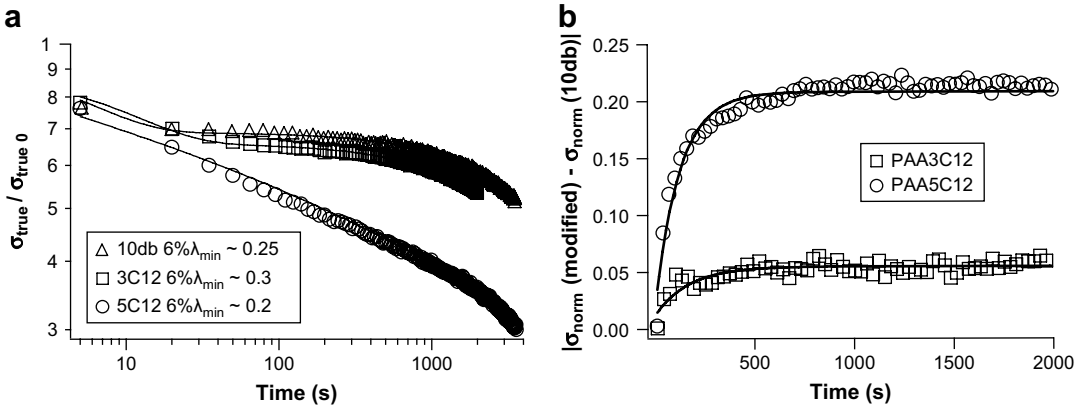

Fig. 12. a. Relaxation of the PAA10 db, PAA3C12 and PAA5C12 hydrogels. b. Same data for the PAA3C12 and PAA5C12 normalized by the relaxation of the 10 db gel.

more progressive for the hydrophobically modified gels, leading to a higher maximal extensibility of the network.

This can be explained by the high density of hydrophobic clusters in the modified gels [29]. Assuming an isotropic distribution of these clusters, the distance between two micelles should be roughly 200 Å. Since the typical chain size between two cross-links is 150 Å, the structure of the network can be schematically envisioned as in Fig. 15.

The hystereses and relaxation experiments suggest that the screening of the same charge interactions by the hydrophobic clusters is not complete and does not prevent the formation of ionic aggregates. The long relaxation time, attributed to the ionic clusters, is still observed and identified for all systems.

From the results of all the experiments, we can suggest a possible molecular mechanism for these hydrophobically modified hydrogels undergoing compression. The fact that J_m is shifted to higher values in the hydrophobically modified hydrogels could mean that hydrophobic micelles are not acting as additional cross-links when the sample is deformed (this is confirmed by the fact that at very low strain rates, no significant difference is observed during loading of both gels, since the time of the experiment is very long compared to the lifetime of the hydrophobic clusters).

On the other hand, the presence of these hydrophobic clusters perturbs the formation of the ionic clusters observed in the polyelectrolyte hydrogels which are more effective in terms of strain hardening, leading to a net increase in the maximum extensibility of the modified hydrogels.

To explain the unloading behaviours, similar to the plastic deformation of a thermoplastic, we can make the hypothesis that the compression of the sample at large strain leads to the formation of "anisotropic" or oriented micelles, once the initially isotropic micelles are "broken" by the stress applied on the sample. These anisotropic micelles are mainly formed with hydrophobic groups from the chains perpendicular to the compression direction, close to one another (see Fig. 16). When these micelles are formed, they are relatively stable and prevent the gel from going back immediately to its initial shape when unloaded.

Our initial motivation for introducing the hydrophobic clusters was to explore a potential mechanism of mechanical reinforcement of the gel and in particular to obtain higher fracture toughness. Preliminary fracture experiments do not suggest spectacular effects and it may be that the characteristic time scales at which the dissipative processes occur during the formation and breakup of the clusters is not active at the tip of a propagating crack where strain rates are typically high. It is however surprising that the nearly plastic deformation observed at large strains for the PAA5C12 hydrogel does not slow down much a propagating crack by relaxing the high stresses present at its tip.

It is also honest to point out that our interpretation of the hysteretic phenomena occurring at large strains remains rather speculative since we did not perform any structural studies under strain. The underlying reason is however that the relatively short relaxation times of the aggregation processes may be too short to capture a structure with a scattering experiment. We feel

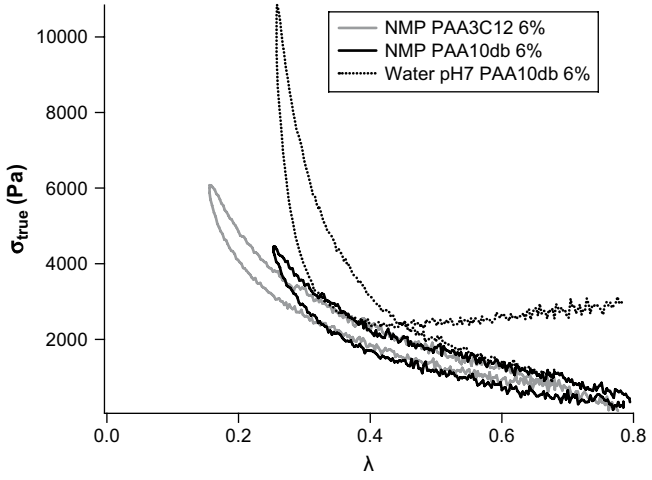

Fig. 13. True compressive stress versus lambda for NMP 6% gels (straight lines, black: 10 db, grey: 3C12). In dotted lines, the PAA10 db in water at the same concentration.

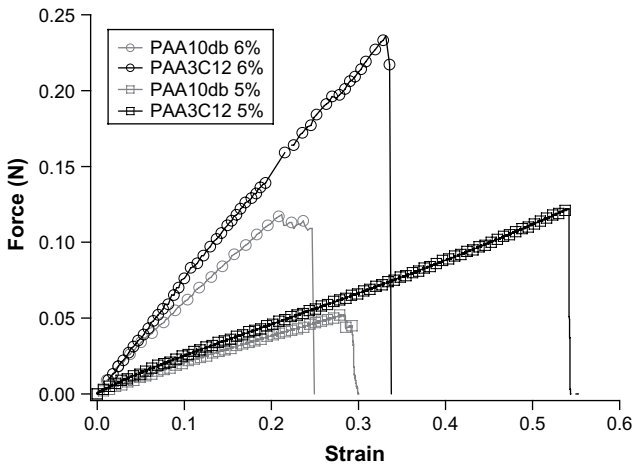

Fig. 14. Fracture experiments force versus strain curves for the three types of notched samples of gels at two concentrations.

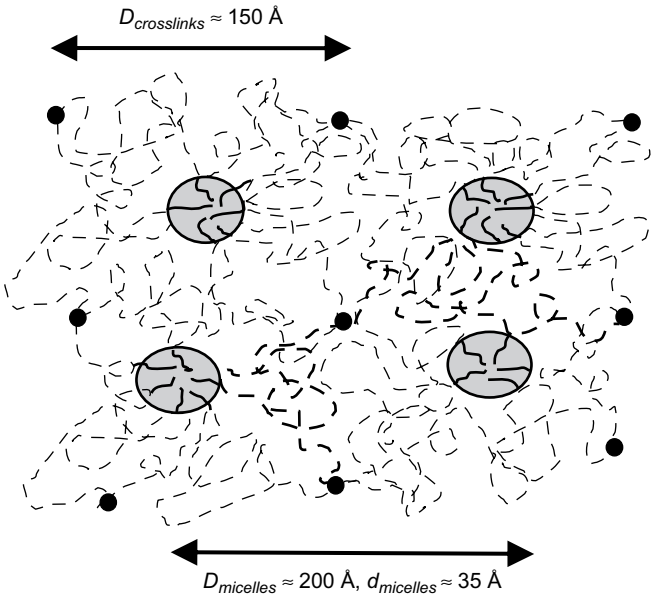

Fig. 15. Structure of the hydrophobic network with the typical distances between chemical cross-links and clusters (D). $d_{micelles}$ is the average diameter of the hydrophobic cluster.

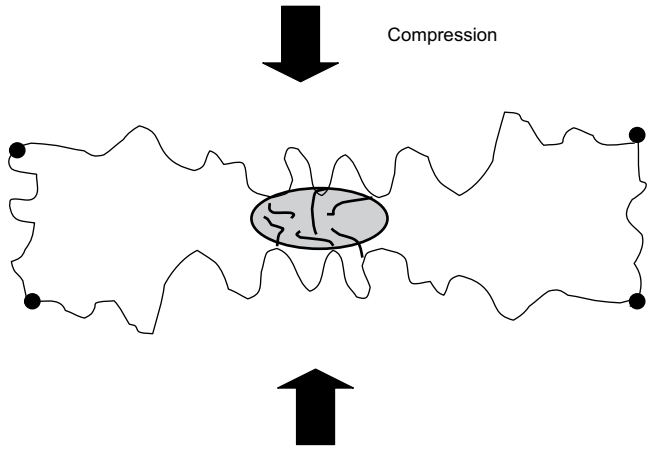

Fig. 16. Formation of anisotropic micelles during compression of a hydrophobically modified hydrogel.

nevertheless that our molecular interpretation is fully consistent, if not unique, with the observed macroscopic behaviour.

5. Conclusion

In this paper we demonstrated the existence of two strongly coupled dissipative mechanisms during the large strain deformation of hydrophobically modified polyelectrolyte hydrogels. One mechanism is inherent to the charged nature of the main polymer network: it is probably due to the aggregation of backbone chains as previously argued [17] whereas the second is related to the hydrophobic clusters and may be caused by their reversible association.

This dissipative mechanism due to the hydrophobic clusters strongly affects the macroscopic behaviour of these materials, both in the linear regime of deformation (great increase in the loss modulus) and at large strains. While the dissipative mechanism is independent of strain when the deformation is approximately below 100%, it becomes very strongly strain and strain rate dependent above this limit. Furthermore, both mechanisms due to clustering are strain rate dependent but the lifetime of the ionic clusters is much longer so that only the effect of ionic clusters are visible at low strain rates, while at high strain rates, both dissipative mechanisms are active. The presence of these dissipative mechanisms at high strains should be contrasted with the much more elastic behaviour observed at small strains and plays a role for the strength of the gels. We also showed that the presence of hydrophobic clusters improves the fracture toughness without changing its elastic modulus suggesting that the introduction of viscous dissipative mechanism is indeed a viable strategy to toughen hydrogels.

Acknowledgment

We would like to thank Denis Valet (PMMH, ESPCI) for his precious help in designing and building the fracture mould. We also would like to thank Hugh Brown and Jean François Joanny for insightful discussions.

References

[1] Hoffman AS. Advanced Drug Delivery Reviews 2002;54:3–12.
[2] Hoare TR, Kohane DS. Polymer 2008;49:1993–2007.
[3] Peppas NA, editor. Hydrogels in medicine and pharmacy. CRC; 1986.
[4] Durmaz S, Okay O. Polymer 2000;41:3693–704.
[5] Cicek H, Tuncel A. Journal of Polymer Science Part A-Polymer Chemistry 1998;36:527–41.
[6] Jabbari E, Nozari S. European Polymer Journal 2000;36:2685–92.
[7] Skouri R, Schosseler F, Munch JP, Candau SJ. Macromolecules 1995;28:197–210.
[8] Okay O, Sariisik SB, Zor SD. Journal of Applied Polymer Science 1998;70:567–75.
[9] Muniz EC, Geuskens G. Macromolecules 2001;34:4480–4.
[10] Okay O, Durmaz S. Polymer 2002;43:1215–21.
[11] Breedveld V, Nowak AP, Sato J, Deming TJ, Pine DJ. Macromolecules 2004; 37:3943–53.
[12] Van den Bulcke AI, Bogdanov B, De Rooze N, Schacht EH, Cornelissen M, Berghmans H. Biomacromolecules 2000;1:31–8.
[13] Ozmen MM, Okay O. Polymer Bulletin 2004;52:83–90.
[14] Webber RE, Creton C, Brown HR, Gong JP. Macromolecules 2007;40:2919–27.
[15] Webber RE, Shull KR. Macromolecules 2004;37:6153–60.
[16] van Vliet T, Walstra P. Faraday Discussions 1995;101:359–70.
[17] Miquelard-Garnier G, Creton C, Hourdet D. Soft Matter 2008;4:1011–23.
[18] Clark AH, Rossmurphy SB. Advances in Polymer Science Adv Polymer Science 1987;83:57–192.
[19] Baumberger T, Caroli C, Martina D. Nature Materials 2006;5:552–5.
[20] Tanaka Y, Kuwabara R, Na YH, Kurokawa T, Gong JP, Osada Y. Journal of Physical Chemistry B 2005;109:11559–62.
[21] Tanaka Y, Fukao K, Miyamoto Y. The European Physical Journal E 2000;3:395–401.
[22] Haraguchi K, Li HJ. Macromolecules 2006;39:1898–905.
[23] Huang T, Xu HG, Jiao KX, Zhu LP, Brown HR, Wang HL. Advanced Materials 2007;19:1622.
[24] Tanaka Y. Europhysics Letter 2007;78:56005.
[25] Brown HR. Macromolecules 2007;40:3815–8.
[26] Lake GJ, Thomas AG. In: Gent AN, editor. Engineering with rubber. Munchen: Hanser; 1992. p. 95–128.
[27] Lake GJ, Thomas AG. Proceedings of the Royal Society of London A 1967;A300:108–19.
[28] Shalaby S, McCormick C, Butler GG. Water soluble polymers, synthesis, solution properties and applications, vol. 467; 1991.
[29] Miquelard-Garnier G, Demoures S, Creton C, Hourdet D. Macromolecules 2006;39:8128–39.
[30] Podhajecka K, Prochazka K, Hourdet D. Polymer 2007;48:1586–95.
[31] Iliopoulos I, Wang TK, Audebert R. Langmuir 1991;7:617–9.
[32] Hashidzume A, Morishima Y. In: Tripathy SK, Kumar J, Nalwa HS, editors. Handbook of polyelectrolytes and their applications. California: ASP; 2002.
[33] Cram SL, Brown HR, Spinks GM, Hourdet D, Creton C. Macromolecules 2005;38:2981–9.
[34] Dobrynin AV, Rubinstein M. Macromolecules 2000;33:8097–105.
[35] Patrickios CS, Georgiou TK. Current Opinion in Colloid and Interface Science 2003;8:76–85.
[36] Gholap SG, Jog JP, Badiger MV. Polymer 2004;45:5863–73.
[37] Magny B, Lafuma F, Iliopoulos I. Polymer 1992;33:3151–4.
[38] Boileau S, Mazeaud-Henri B, Blackborow R. European Polymer Journal 2003;39:1395–404.
[39] Josse G, Sergot P, Dorget M, Creton C. Journal of Adhesion 2004;80:87–118.
[40] Rivlin RS, Thomas AG. Journal of Polymer Science 1953;10:291–318.
[41] Baumberger T, Caroli C, Martina D. European Physical Journal E 2006;21: 81–9.
[42] Gent AN. Rubber Chemistry and Technology 1996;69:59–61.